

NPS ARCHIVE  
1958  
MORIN, G.

THE INFLUENCE OF ANTI-PITCHING  
FINS ON SHIP MODEL BENDING MOMENTS

GENE D. MORIN  
AND  
WILLIAM E. TRUEBLOOD

DUDLEY KNOX LIBRARY  
NAVAL POSTGRADUATE SCHOOL  
MONTEREY CA 93943-5101









THE INFLUENCE OF ANTI-PITCHING FINS ON SHIP MODEL  
BENDING MOMENTS

by

GENE D. MORIN, Lieutenant, United States Navy

B.S., U.S. Naval Academy

(1950)

and

WILLIAM E. TRUEBLOOD, Lieutenant, United States Navy

B.S., U.S. Naval Academy

(1953)

SUBMITTED IN PARTIAL FULFILLMENT  
OF THE REQUIREMENTS FOR THE  
DEGREE OF NAVAL ENGINEER  
AND THE DEGREE OF  
MASTER OF SCIENCE IN NAVAL ARCHITECTURE  
AND MARINE ENGINEERING

at the

MASSACHUSETTS INSTITUTE OF TECHNOLOGY

May 1958





## ABSTRACT

### THE INFLUENCE OF ANTI-PITCHING FINS ON SHIP MODEL BENDING MOMENTS

by

Gene D. Morin and William E. Trueblood

Submitted to the Department of Naval Architecture and Marine Engineering on May 26, 1958 in partial fulfillment of the requirements for the degree of Naval Engineer and the degree of Master of Science in Naval Architecture and Marine Engineering.

The object of this thesis was to investigate the effect of anti-pitching bow fins on the bending moment of a destroyer model running in regular ahead waves. The necessity for a stable platform in guided missile vessels prompted this investigation.

The experimental data was obtained by installing a flexure bar in a modern destroyer model (5.8 ft) which had been cut at the amidship section. Bending moment was measured at the amidship section using electrical resistance type strain gages mounted on the flexure bar and wired to a Brush Analyzer and Direct Inking Oscillograph. The model was towed at various constant towing forces in waves, with and without bow fins, which were of the rectangular flat plate type located at keel depth.

The experimental data indicated that (1) the influence of anti-pitching fins, at the wave length and speed combinations most likely to be met in service, was to increase both hogging and sagging bending moments, (2) the measured bending moments were well below the calculated static values, and (3) maximum bending moment occurred when the wave nodal point was at the longitudinal center of gravity.

Thesis Supervisor: M. A. Abkowitz

Title: Associate Professor of Naval Architecture



Cambridge 39, Massachusetts  
May 26, 1958

Secretary of the Faculty  
Massachusetts Institute of Technology  
Cambridge 39, Massachusetts

Dear Sir:

In accordance with the requirements for the Degree of Naval Engineer and the Degree of Master of Science in Naval Architecture and Marine Engineering, we herewith submit a thesis entitled: "The Influence of Anti-Pitching Fins on Ship Model Bending Moments."

Respectfully,

GENE D. MORIN  
Lieutenant, United States Navy

WILLIAM E. TRUEBLOOD  
Lieutenant, United States Navy



## TABLE OF CONTENTS

	<u>Page</u>
Abstract	i
Letter of Transmittal	ii
Table of Contents	iii
List of Figures	iv
List of Symbols	1
I. Introduction	2
II. Procedure	5
III. Results	13
IV. Discussion of Results	22
V. Conclusions	30
VI. Recommendations	31
VII. Bibliography	32
VIII. Appendix	33
A. Details of Procedure	34
B. Equipment Data	35
C. Summary of Data and Calculations	36
D. Sample Calculations	38
E. Drawings and Photographs	45
F. Original Data	52



## LIST OF FIGURES

### Figure

- I. Speed Reduction Curves
- II. Total Dynamic Bending Moment vs. Model Speed for  $\lambda/L = 0.75$
- III. Total Dynamic Bending Moment vs. Model Speed for  $\lambda/L = 1.00$
- IV. Total Dynamic Bending Moment vs. Model Speed for  $\lambda/L = 1.25$
- V. Total Dynamic Bending Moment vs.  $\lambda/L$  for Model Speed of 0.5 knots
- VI. Total Dynamic Bending Moment vs.  $\lambda/L$  for Model Speed of 1.0 knots
- VII. Total Dynamic Bending Moment vs.  $\lambda/L$  for Model Speed of 1.4 knots
- VIII. Percent of Maximum Bending Moment vs. Location of Wave Profile
- IX. Sketch of Model Showing Flexure Bar Installation
- X. Sketch of Model Showing Bow Fin Installation
- XI. Diagram of Strain Gage Installation
- XII. Method of Strain Gage Calibration
- XIII. Photograph of Midship Section Showing Flexure Bar and Towing Bracket
- XIV. Photograph of Instrument Setup
- XV. Photograph of Model Fully Rigged in Tow Tank
- XVI. Photograph of Bow with Anti-Pitching Fins Installed





## LIST OF SYMBOLS

$a$	Wave height, in inches, or as fraction of wave length
$k_y$	Radius of gyration, in inches
$L$	Length between perpendiculars, in feet
$T_e$	Period of wave encounter, in seconds
$T_p$	Natural period of pitching, in seconds
$V_s$	Still water speed, in knots
$V_v$	Speed of ship or model in waves, in knots
$V_w$	Wave speed, in knots
$\lambda$	Wave length, in feet, or as a fraction of the model length



## I. INTRODUCTION

The design of steel ships for proper longitudinal strength has been an important problem in the field of naval architecture. Design of midship sections has been done more in a comparative manner with previous successful designs. The ultimate test of this method would be a failure of a vessel due to inadequate longitudinal strength. Since this is undesirable, attempts have been made to evaluate the estimated bending moments by measuring actual bending moments in ship models. It must be realized that in order to approximate actual bending moments, the actual loading conditions and wave phenomena must be duplicated. Accomplishment of the first is possible; however, the task of duplicating wave conditions is difficult, but a field in which much research is being carried on.

The impact of the guided missile program on the modern navy has imposed a demanding requirement on ship stabilization. The first guided missile destroyer, U.S.S. GYATT (DDG-1), has anti-roll fins installed. In anticipation of the use of anti-pitching fins on future guided missile destroyers, it was considered appropriate to investigate the effect of these fins on the bending moment induced in a destroyer ship model in regular ahead seas.



Measurement of bending moment has been done by measuring ship deflections with an electrical pickup and secondly, by instrumenting with strain gages. The success and simplicity of the strain gage method as described in reference (9) indicated this method to be appropriate for this thesis.

Initially it was decided to test the destroyer model at full load condition in regular ahead waves of the proportions  $\lambda/L$  of 0.50, 0.75, 1.00, and 1.25 with the wave height  $1/20$  of the wave length. However, difficulty with the wave generator eccentricity adjustment motor made it necessary to eliminate the  $\lambda/L$  of 0.50. Still water speeds of 10 knots, 15 knots, 20 knots, and 27 knots were selected to cover the speed range of a destroyer.

The model was patterned after a modern United States destroyer, sawed in half at the midship section and held together with an aluminum flexure bar instrumented with four strain gages at amidships. Bending moment, wave profile and speed over the ground were measured for the various wave and speed combinations. After this data was obtained, the model was equipped with flat bow fins at keel depth and towed at the selected still water speeds. Again bending moment, wave profile and speed were measured for the different wave and speed combinations.



High speed motion pictures were taken of all runs. It was hoped that pitch measurement could be accomplished in this manner. However, due to difficulties which will be mentioned later, only a qualitative study of motion could be made.





## II. PROCEDURE

### 1. Construction of Model

In an effort to reduce the consumption of time and money a letter was written to the Commanding Officer and Director, David Taylor Model Basin, inquiring as to the availability of a suitable destroyer model for this thesis. Return correspondence indicated that an adequate model was not available, and that the cost to procure such a model from a private firm would be about \$350.00. In view of these circumstances, it was decided to build a model using the facilities of the M.I.T. Model Shop. The lines were patterned after a modern United States destroyer.

Standard ship modeling procedure was used, employing one and one-quarter inch thick sugar pine lifts. The model was hollowed out to a  $3/4$ " wall thickness and a  $1\frac{1}{4}$ " bottom thickness. Two fir mounting blocks ( $3/4$ " x  $2\frac{1}{4}$ ") for the flexure bar were glued to the bottom lift, leaving a two inch gap at the midship section for the strain gages. The flexure bar, selection and location of which is described later, was attached to the mounting blocks by use of adequate screws. The model was then sawed through at the midship section, using a small hand saw. The flexure bar preserved the rigidity and alignment of the two model halves.



All bare wood was covered with three coats of shellac, this being especially necessary at the midship section where water penetration could cause lift separation.

Installation of the flexible expansion joint is best described by referring to Figure IX. Scotch-brand plastic tape was used (0.010 inches thick). The adhesive of the tape itself was used for bonding. The groove was cut by use of a small hand miter saw. After insertion of the scotch tape, this groove was filled with plastic wood. The model was then given two coats of white enamel to aid in photography.

The towing bracket was installed so that the axis of pitch would be at the scaled down longitudinal and vertical centers of gravity of the full scale ship. The bracket provided freedom in pitch and the tow tank apparatus provided freedom in heave and surge.

By pivoting each model half on a knife edge prior to installation of the expansion joint, the longitudinal center of gravity of each bare hull half was determined. The center of gravity of the flexure bar and cover plates was measured, and then by standard moment calculation, the location of ballast was ascertained so that the LCG of each hull section would correspond to that of the full scale ship. By pivoting the completely assembled model, it was necessary to shift only a small amount of ballast to obtain the proper LCG for



the complete model. Therefore, it is felt that the location of LCG of each section closely approximates that of actual operating conditions.

## 2. Design and Installation of Anti-Pitching Fins

In the interest of time it was decided to use fins similar to those described in reference (10). The fins are essentially flat rectangular plates,  $1/8$ " thick, shaped at the leading and trailing edges. The span of each fin is 2.51" and the chord is 2.0". The planform area is 10.04 in<sup>2</sup> or about 2.5% of the load waterplane area.

The fins were machined from a solid brass block, which, on the centerline, was shaped to match the contour of the hull. After the hull was recessed in the desired location, the fins were secured by means of threaded rods which extended through the hull. See Figure X for details of the installation.

## 3. Instrumentation

Using the intended speeds and wave conditions, the frequency of encounter for each combination was calculated. It was determined that the maximum expected frequency of encounter would be about 3.5 cps. A safety factor of five was chosen, and a minimum size flexure bar calculated so that the bar's natural frequency would be at least five times the maximum frequency of encounter. This minimum





size permitted use of the 1/2" x 1" x 41.75" aluminum flexure bar which had been used in reference (9). This bar had strain gages installed as shown in Figure XI. A continuity and resistance check indicated these strain gages to still be good.

As discussed in reference (5), the total bending moment is a sum of the moments due to vertical and compressive forces. Location of the flexure bar at the neutral axis of the mid-ship section corresponds closely to the centroidal axis about which the compressive forces act. Therefore, the neutral axis of the bar was located at the scaled down neutral axis of the ship.

The radius of gyration and natural pitching period of the model were then determined as outlined in appendices D-4 and D-5, respectively.

The calibration of the strain gages was carried out as shown in Figure XII. The forward section of the model was allowed to overhang the table and the after section weighted down. Successive increments of moment were then applied by a pulley system and the recorder reading noted with each increment. The after section was then allowed to overhang and the forward section supported; another calibration being made. These values were used to evaluate subsequent bending moment readings.





Detailed instrument data is listed in appendix B. Instruments were set up as follows:

a. A Sanborn 127 recorder was connected to the integrator, Eput meter and oscillator combination to measure the speed of the model in waves.

b. A Sanborn 127 recorder was connected to a capacitance probe to measure wave profile during the runs.

c. The strain gage output was fed into a Brush Universal Analyzer. The signal from this analyzer was then fed into one channel of a two channel Brush Direct-Inking Oscillograph.

d. The electric eye located at the approximate mid-length of the tow tank was connected to the second channel of the oscillograph to provide a method of matching the wave profile and bending moment data tapes. Details of this procedure are covered in appendix A.

#### 4. Data Runs

Only two persons were required to make the data runs. The step by step procedure was as follows:

a. With the strain gage output lead disconnected from the model, the four desired still water speeds were obtained, without fins.

b. The wave generator was set up for the desired wave length and height.



c. The strain gage output lead was connected at the model and led out to a pole. This pole was used to manually support the output lead cable as one man followed the model down the tank during each run.

d. The wave generator and recording instruments were activated. A still water bending moment was thus recorded prior to the waves reaching the model on each run.

e. Just prior to the wave pattern reaching the far end of the tank, the model was released and data collected.

f. The model was returned to the far end of the tank and the output lead disconnected.

g. One man released the model at the same speed and wave condition as above. The other person, using a high speed motion picture camera, took pictures of the model through the glass wall of the tow tank.

h. This procedure was repeated for all wave and speed conditions.

i. Three times during the data runs the model was removed from the water and reference strain gage readings taken with the bow overhanging a table, the stern overhanging, and the model supported all along the keel.

The anti-pitching fins as shown in Figure X were installed, ballast being removed to keep the displacement and LCG of the forward section unchanged. The above steps were



altered in an attempt to conduct the runs more efficiently. These steps were as follows:

a. With the strain gage output lead disconnected from the model, the four desired still water speeds were obtained, with fins.

b. The wave generator was set up for the desired wave length and height, and activated.

c. One man released the model and the other person took pictures of the model, using a high speed motion picture camera. This time the pictures were taken from the level of the tank wall (not through the glass wall). Pictures were taken for all different speed and wave combinations.

d. The strain gage output lead was connected at the model and led out to a pole. Data was then collected for all different speed and wave combinations. Thus the inconvenience and zero shift of the analyzer as encountered in the "no fin" runs was eliminated.

e. The model was removed from the water and reference strain gage readings taken with the bow overhanging a table and then with stern overhanging. The model was then placed in the water and a still water reading taken. Knowing the moment of each hull section, it was then possible to establish a zero reference and obtain the still water bending moment. Previous assumptions that a zero reference could be established by supporting the model all along proved





fallacious because of the small distortion introduced when cutting the model in half.

f. The strain gages were once more calibrated using successive increments of moment. An average of the pre-run and post-run calibration readings was used to evaluate bending moment.

An attempt was made to check the natural pitching period of the model by manually oscillating the model in still water and examining the period of bending moment as recorded on the tape. However, the pitching of the model damped so quickly that no pitching period could be determined.





### III. RESULTS

The results of the bending moment comparison are presented in the following graphs:

#### Figure I - Speed Reduction Curves

Model speed vs. wave length is plotted to illustrate the speed reduction at a constant towing force. The 15 knot curve has been omitted to permit easier reading of the graph.

#### Figure II - Total Dynamic Bending Moment vs. Model Speed for $\lambda/L=0.75$

Hogging and sagging bending moment for the model, with and without fins, is plotted.

#### Figure III - Total Dynamic Bending Moment vs. Model Speed for $\lambda/L=1.00$

#### Figure IV - Total Dynamic Bending Moment vs. Model Speed for $\lambda/L=1.25$

#### Figure V - Total Dynamic Bending Moment vs. $\lambda/L$ for Model Speed of 0.5 knots

These cross curves were plotted using the curves of Figures II, III, and IV. They are designed to show the effect of bow fins on bending moment as  $\lambda/L$  increases for a given speed.

#### Figure VI - Total Dynamic Bending Moment vs. $\lambda/L$ for Model Speed of 1.0 knots

#### Figure VII - Total Dynamic Bending Moment vs. $\lambda/L$ for Model Speed of 1.4 knots

#### Figure VIII - Percentage of Maximum Bending Moment vs. Wave Nodal Point Location



FIGURE I  
Speed Reduction Curves

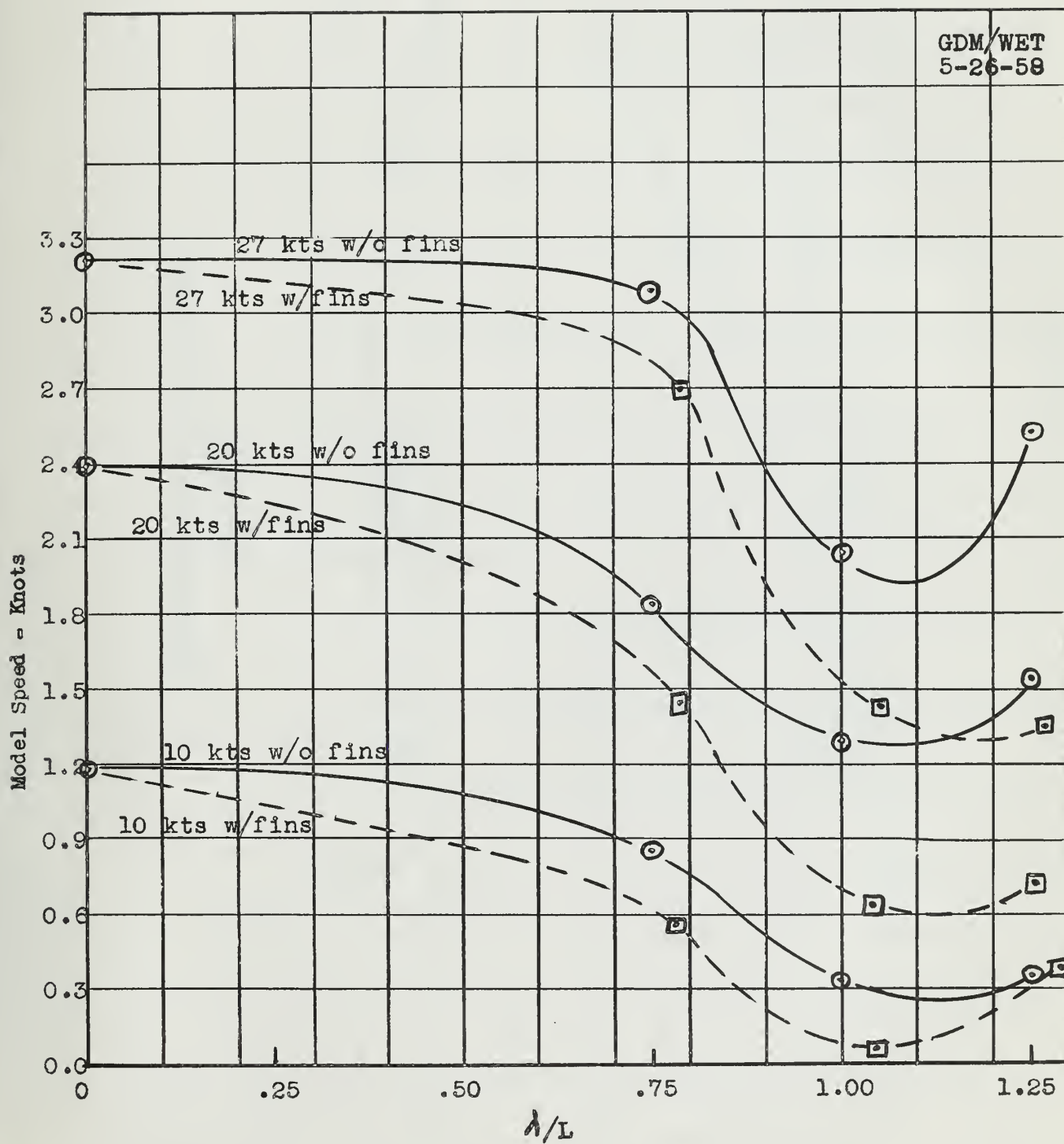




FIGURE II

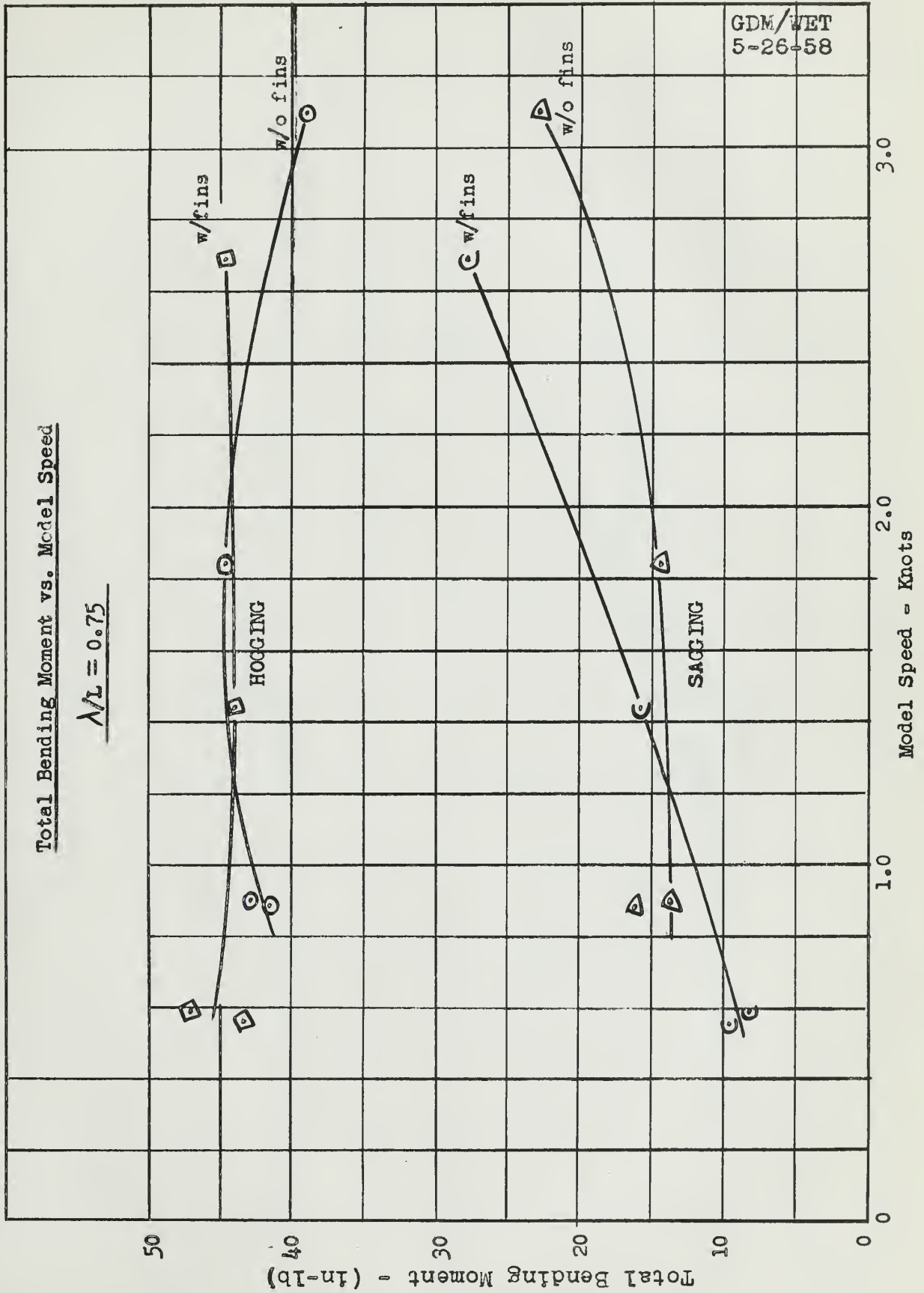




FIGURE III

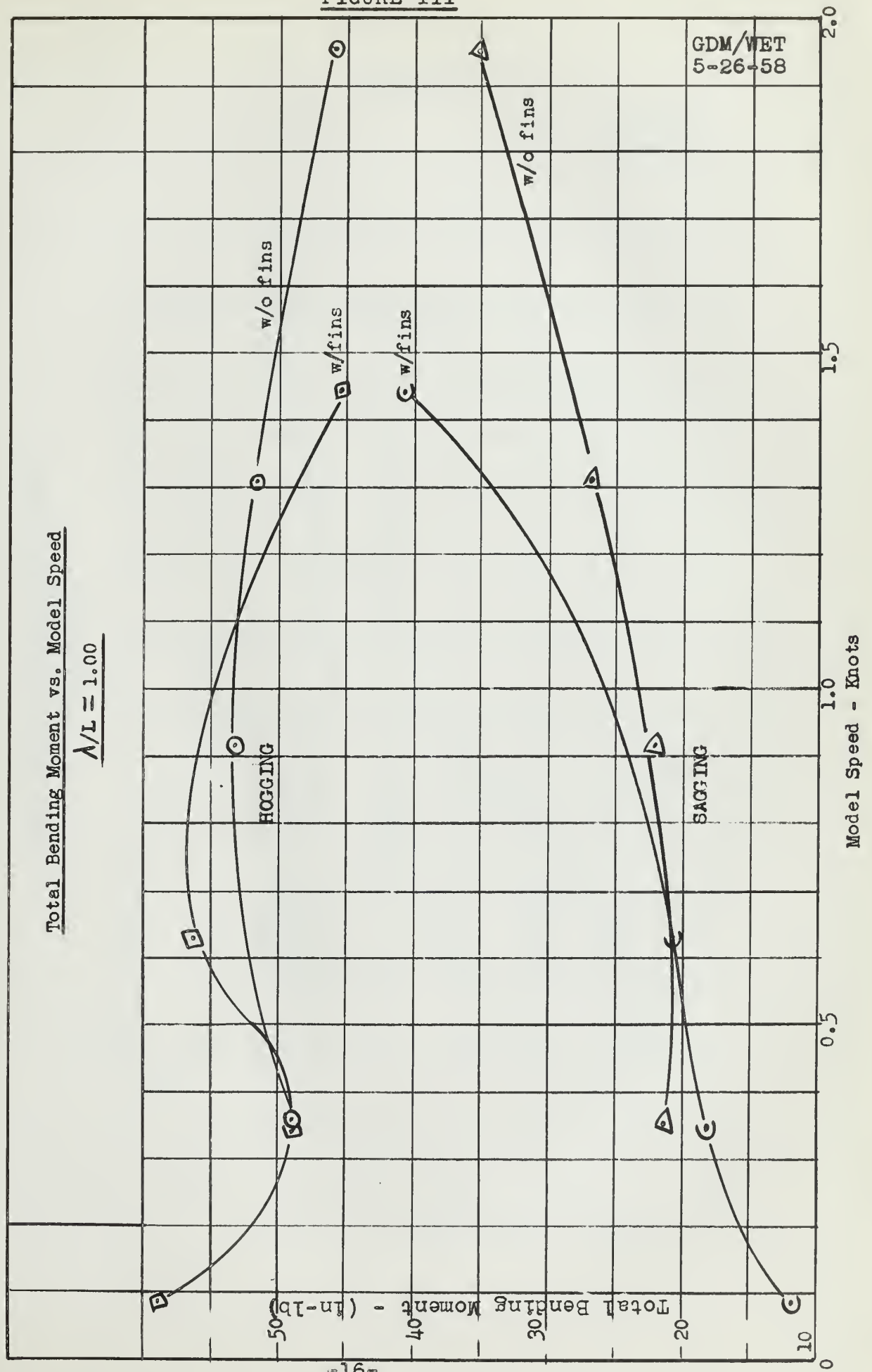






FIGURE IV

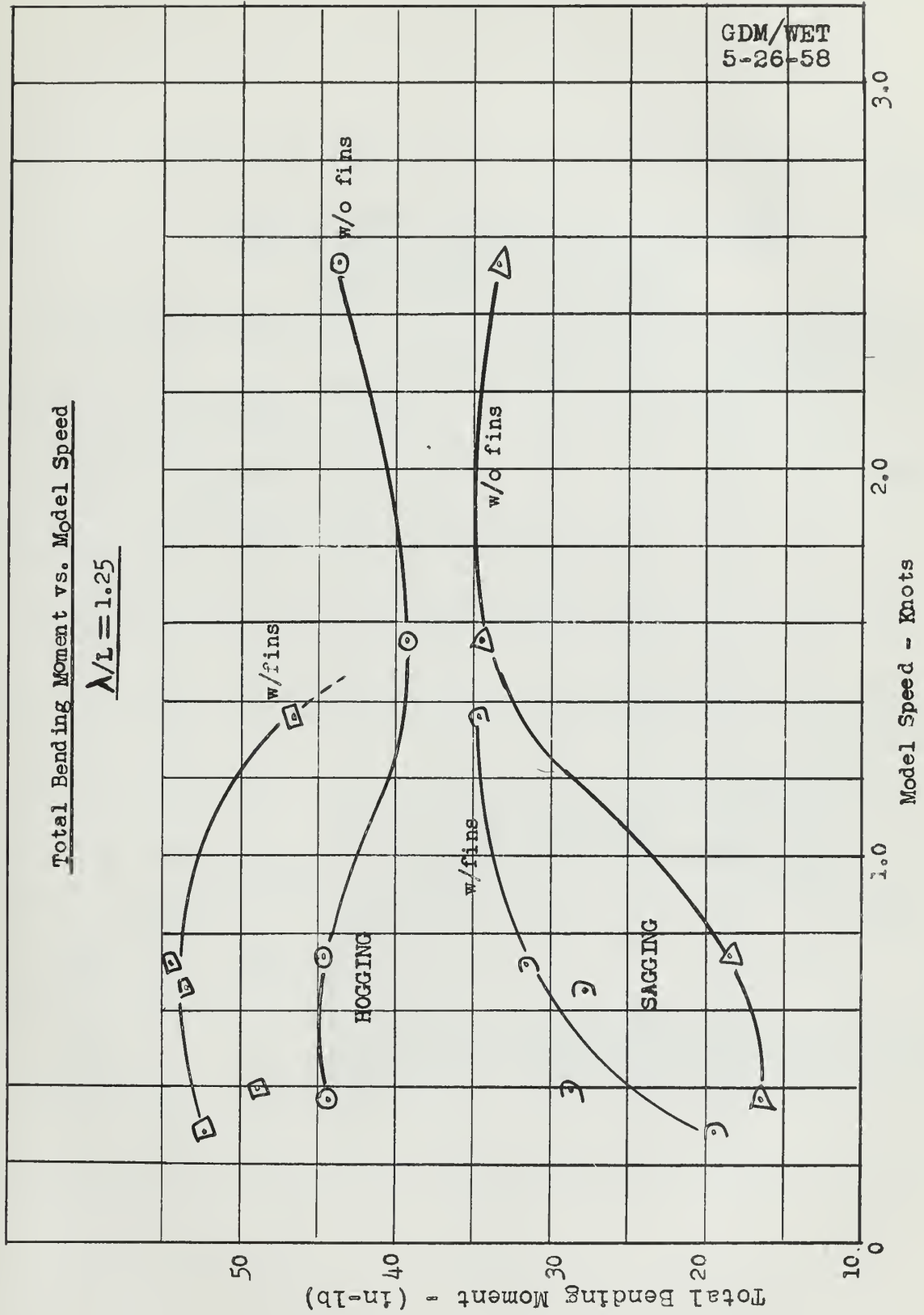




FIGURE V

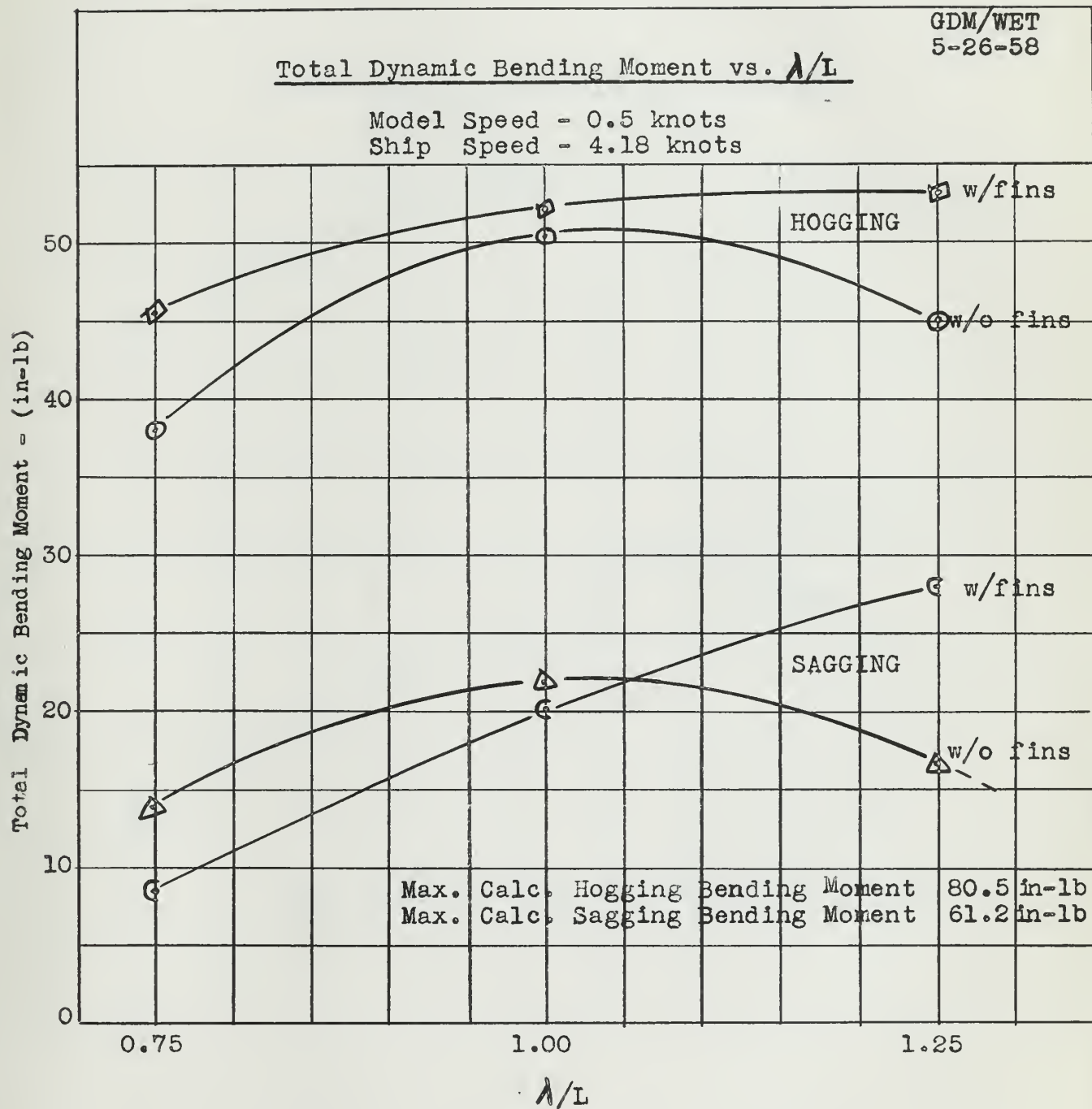




FIGURE VI

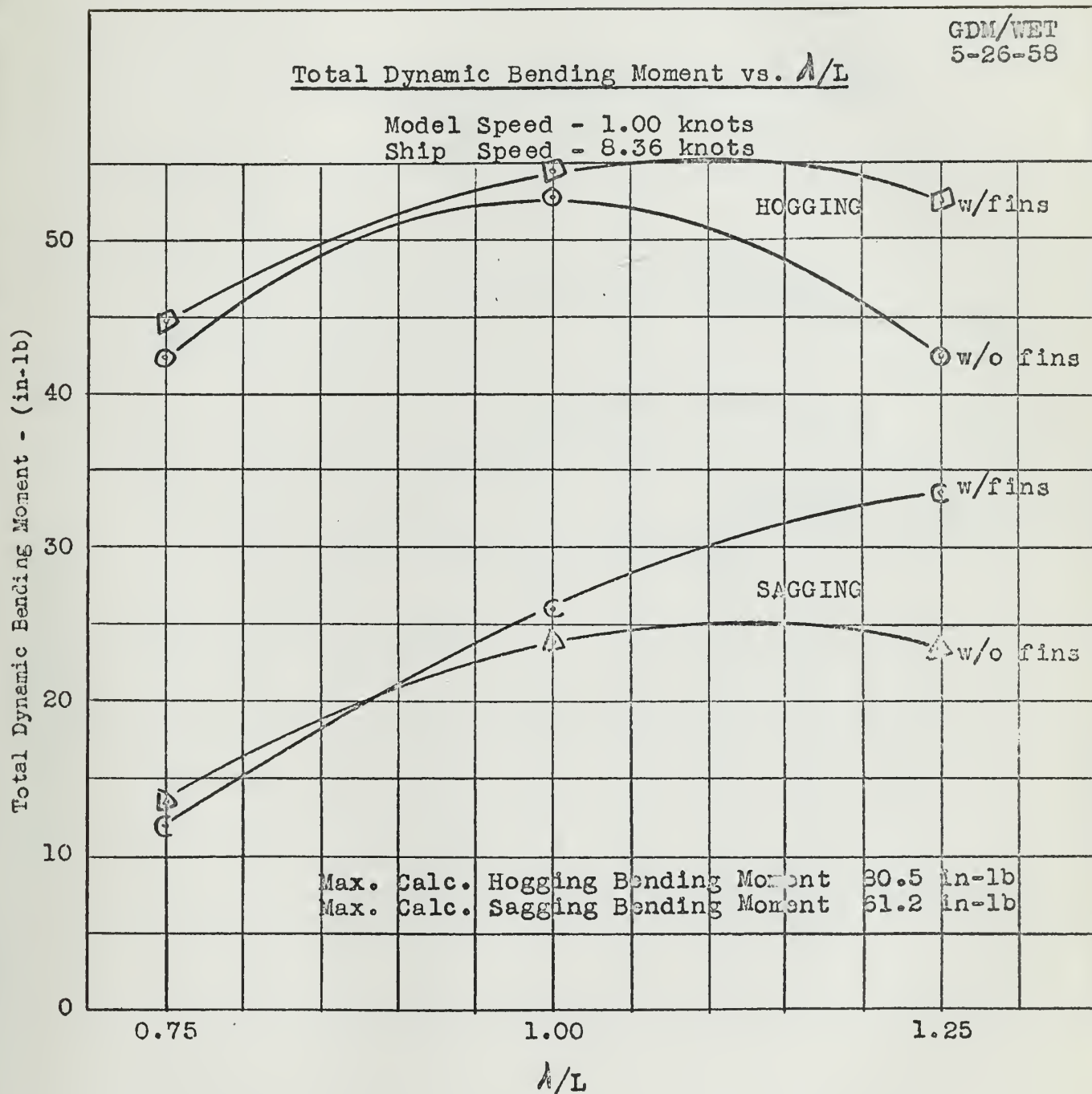




FIGURE VII

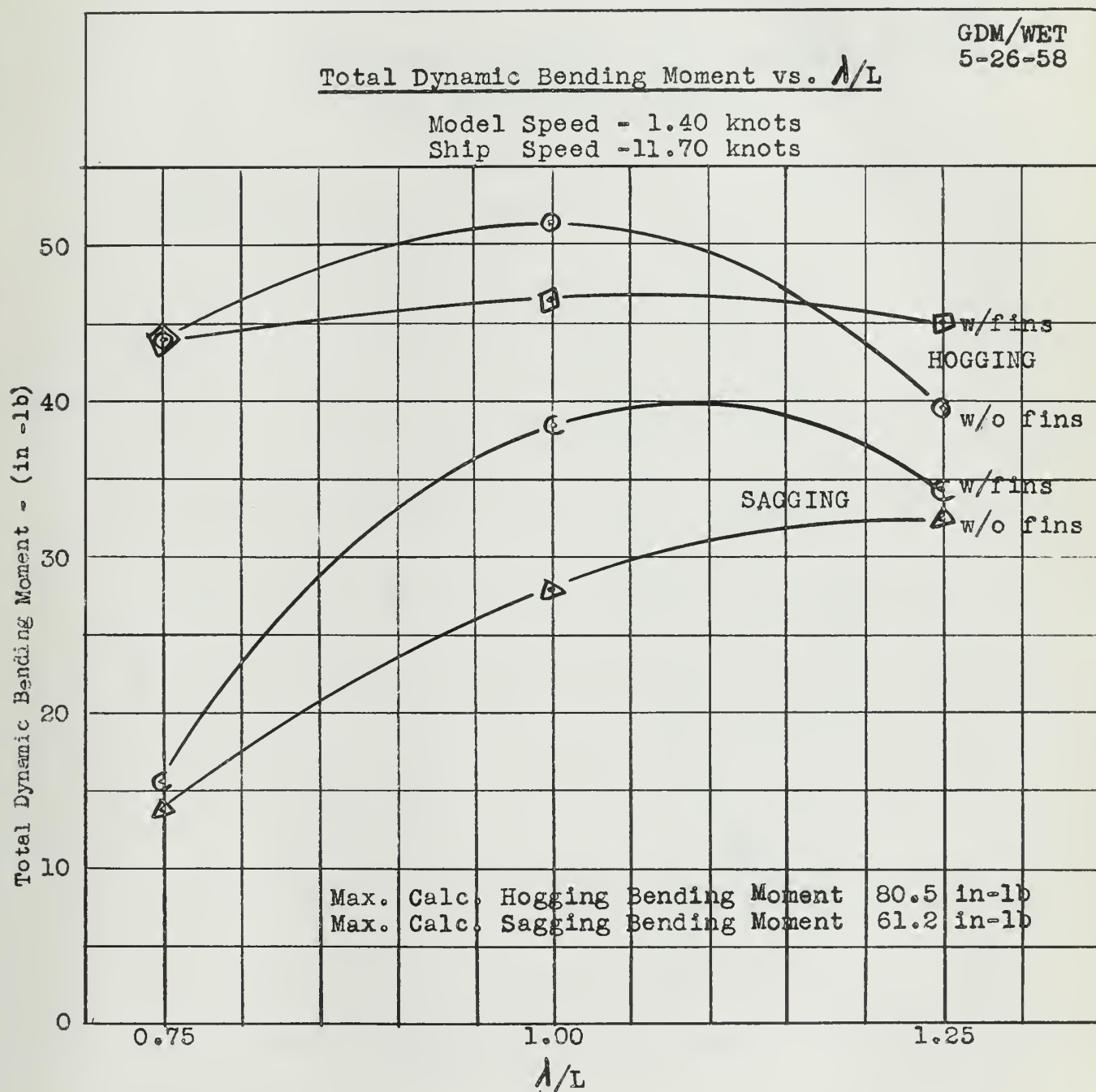
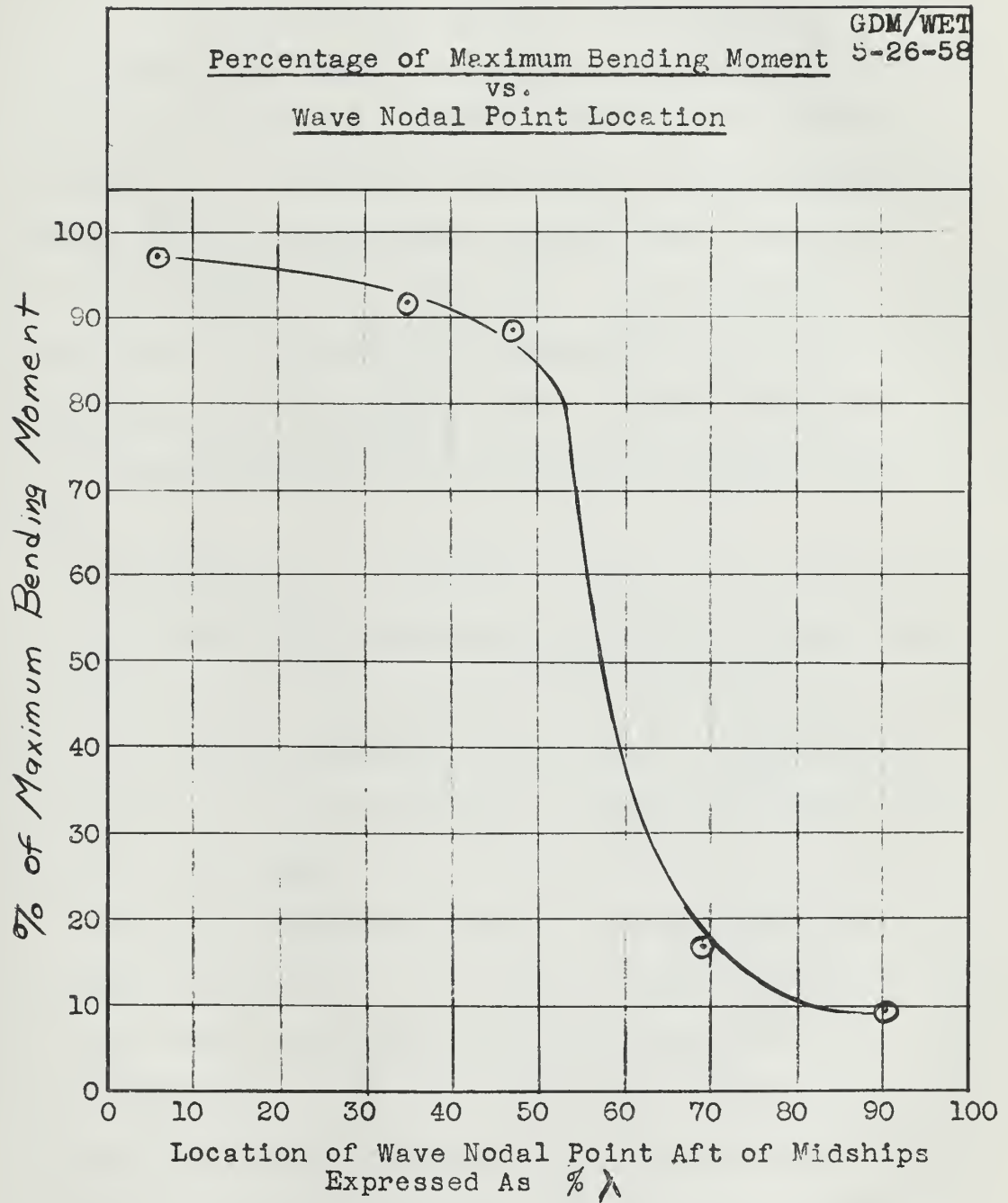






FIGURE VIII





#### IV. DISCUSSION OF RESULTS

##### 1. Speed Reduction

The gravity (falling weight) towing system at the M.I.T. towing tank made it possible to utilize the constant or maintained resistance towing condition as discussed in reference (1). The towing force for a given speed was determined and then maintained constant while towing the model with various wave conditions. This condition of towing for the model is practically equivalent to the ship condition of maintained EHP or propeller RPM. Thus, the duplication of an actual condition that might exist upon the ship is realized.

In reference (1) the speed reduction in waves experienced by a Series 60, Block 0.60 model equipped with bow hydrofoil anti-pitching fins is discussed. For wave length of less than  $0.77L$  the speed reduction with fins is greater than without fins; for wave lengths of greater than this value the opposite is true.

The speed reduction curves for a destroyer type model are shown in figure I. It is readily seen that in all cases the speed reductions experienced with fins are greater than those without fins. As speed increases the difference in the reductions becomes greater except at the lowest speed examined. The speed reductions with fins are therefore in direct contradiction to what one would expect through in-



tuition and also to those reported in reference (1). With a given power it is apparently not possible to achieve a greater speed in waves through the installation of anti-pitching fins, even though the fins might materially reduce the motions. It is recommended that further tests be made on this destroyer model, both with and without fins, at longer wave lengths to further establish the validity of this conclusion.

The relative wave lengths for maximum speed reductions at the 20 and 27 knot conditions do agree with those experienced by the Series 60 model. The maximum speed reduction with fins occurred at a greater wave length than that without fins.

The still water increase in resistance due to installation of the fins may be derived from Table I by comparing towing force. The with fin resistances expressed as a percentage of without fin resistance is as follows:

<u>Speed</u>	<u>Percentage</u>
10	139
15	115
20	112
27	106

These are in conformity with what one might expect because of the relatively larger contribution of frictional resistance at the lower speeds.



## 2. Measurement of Bending Moments

In each plot where total bending moment is the ordinate, the plotted value is the total, i.e., still water bending moment plus or minus the dynamic bending moment, which existed under the specified conditions of wave length, wave height, and speed. In order to plot total bending moment it was necessary to obtain either an accurate zero reference or the value of the bending moment existing under still water conditions. It was found that an accurate value for the former was practically impossible to obtain.

The methods used and discussed in the procedure for obtaining an accurate value of still water bending moment yielded a value which agreed quite well with the calculated value. This value, as obtained by integrating the weight and buoyancy of the ship at the designer's load waterline and then reducing to the model by use of the proper scale factor, was about 19.0 inch-lbs. The measured value was 18.75 inch-lbs with therefore a 1.3% difference.

The static bending moment calculations for the ship poised on a  $1.1\sqrt{L}$  wave predicted a value of 80.45 inch-lbs hogging condition and 61.23 inch-lbs in sagging condition for the model. The maximum measured hogging bending moment was 59 inch-lbs or 73.5% of the calculated; the maximum measured sagging bending moment was 40.7 inch-lbs or 66.3% of the calculated. Thus, the measured values were considerably less than the static calculated values in all cases.





### 3. Effect of Model Speed on Bending Moment for a Given Wave

#### Hogging Bending Moment

- 0.75 w/o fins - Reaches maximum at 1.77 knots(14.8 kts ship speed) and decreases thereafter.
- w/fins - Reaches minimum at 1.77 knots(14.8) and increases thereafter.
- 1.00 w/o fins - Reaches maximum at 1.0 knots(8.36) and decreases thereafter.
- w/fins - Reaches maximum at 0.75 knots(6.27) and decreases thereafter.
- 1.25 w/o fins - Reaches maximum at 0.56 knots(4.68) A point of inflection occurs thereafter. Additional data would be needed to determine if the bending moment then exceeds the initial maximum as model speed is increased.
- w/fins - Reaches maximum at 0.70 knots(5.85) and decreases thereafter.

#### Sagging Bending Moment

- 0.75 w/o fins - Increases with increasing speed  
w/fins - Same
- 1.00 w/o fins - Same  
w/fins - Same
- 1.25 w/o fins - Increases with increasing speed up to 1.8 knots (15.05) and then tends to decrease slightly.
- w/fins - Increases with increasing speed.

The above summary illustrates that no overall conclusion can be drawn about the variation of bending moment with model speed regardless of wave condition. It is believed that the availability of more data would define the curves better and eliminate any possible erratic points. The true value of Figures II, III, and IV is in their use for drawing the cross curves of Figures V, VI, and VII.



#### 4. Effect of Wave Length on Bending Moment for a Given Speed

It might be expected that the installation of anti-pitching fins would influence the bending moment in a given ship in either of two ways. The reduced motions of the ship in waves would result in a more uniform buoyancy distribution with a resulting decreased bending moment or the added moment due to the water acting on the fins as the ship tries to pitch might increase the bending moment. The two must not be considered separately.

A comparison of Figures V, VI, and VII shows that for the lower wave lengths and particularly at the lowest speed, the influence of the fins is to increase the hogging bending moment and decrease sagging, but not to materially change the range, i.e., hogging plus sagging. As the speed and  $\lambda/L$  are increased, the sagging bending moment, both with and without fins, increases; the with fin value increasing at a faster rate until, at the highest speed plotted, the with fin value is greater regardless of wave length.

The value of the hogging bending moment, without fins, is not influenced by speed, but is relatively constant over the range of wavelengths examined. This does not apply to the without fins sagging bending moment. It increases both with speed and  $\lambda/L$ .



It was observed that the model, with the fins installed, did experience considerable slamming as the wave length was increased, with the worst condition existing at  $\lambda/L=1.0$  and the highest speed. The effect of the slamming is to increase the sagging bending moment such that at the higher wave lengths it is greater than that experienced by the bare hull. At a model speed of 1.4 knots and  $\lambda/L=1.08$ , which is close to the worst slamming condition, the sagging bending moment is a maximum. This is certainly what one should expect.

The influence of the fins, at the wave length and speed combinations most likely to be met in service, is to increase both hogging and sagging bending moments, and therefore to materially increase the stress requirements on the hull girder.

#### 5. Relative Positions of Model and Wave Profile for Maximum Bending Moment

Figure VIII has been plotted using the data of Table III. Because of personnel error during the data runs, it was not possible to correlate the wave profile and bending moment data tapes of the "with fin" runs. Initially a plot was made of the percentage of maximum bending moment vs. wave nodal point location relative to amidships. Little correlation was found in this plot. Consequently, the ratio of wave nodal point location relative to amidships/





total wave length was used to plot against percentage of maximum bending moment. This is the plot of Figure VIII. Only hogging moments have been used in this evaluation. More data points would be helpful, of course, but it must be realized that the factor of chance is involved in the electric eye being tripped during a hogging condition and in obtaining a proper scattering of points. From reference (3) it is noted that for static calculations, the maximum bending moment occurs when the wave nodal point is located at the LCG of the ship. Since the LCG of the model was 1.17 inches aft of amidships, it can be concluded that the dynamic measurements agree quite well with static calculations.

## 6. Model Motion

It was initially intended that the pitching motion of the ship be measured by taking high speed motion pictures of the model. For the without fin runs pictures were taken through the glass wall of the tank. It was intended that pitch angle be determined by comparing the waterline inclination with a fixed reference. However, this film had few good frames for motion study.

For the with fin runs a vertical striped dowel was installed at the bow extending upward from the deck. Pictures were taken at right angles to the tow axis and at





a level of the top of the tank wall. This film developed excellently. Pitch angle could be measured at the very slow speeds; however, at high speeds a full cycle of the marker dowel motion was not recorded because of the short time which the model was within the camera field of view. As a result of the above difficulties, a comparison of pitching motion with and without fins could not be made.

It is concluded that high speed motion pictures taken from an oblique angle to the tow axis would be valuable for a qualitative study of model motion. For quantitative results, it is recommended that a gyro and accelerometer system be installed to measure pitch and heave.

#### 7. Accuracy of Measurement

Measurement was within the following limits:

- a. Weight -  $1/32$  lb or 1.25%
- b. Bending Moment Tape -  $1/4$  unit or 0.83%
- c. Speed Tape -  $1/4$  unit or 1.25%
- d. Wave Profile Tape -  $1/4$  unit or 1.25%



## V. CONCLUSIONS

From the foregoing discussion it is concluded that:

1. The influence of anti-pitching fins, at the wave length and speed combinations most likely to be met in service, is to increase both hogging and sagging bending moments. Therefore, the stress requirements on the hull girder are increased.

2. In a short wave at a slow speed the total range of bending moment is not increased by the installation of fins.

3. Hogging bending moments are relatively constant with respect to speed. Sagging bending moments are directly proportional to speed.

4. The measured bending moments are well below the calculated static values.

5. Maximum bending moment occurs when the wave nodal point is at the longitudinal center of gravity.

6. The hogging bending moment, without fins, is a maximum at  $\lambda/L = 1.0$ .



## VI. RECOMMENDATIONS

1. Additional wave lengths and still water speeds should be used to provide data for corroborating the present bending moment curves.

2. The model should be instrumented with a gyro and accelerometer system to measure pitch and heave; and thus provide some accurate means of measuring the effect of bow fins on a destroyer model.

3. A Sanborn four channel recorder should be used to promote efficiency during data runs and accuracy of matching wave profile and bending moment tapes.

4. A series of fins should be developed for use in conjunction with recommendation 2.

5. Speed reduction should be further studied in conjunction with recommendation 1.

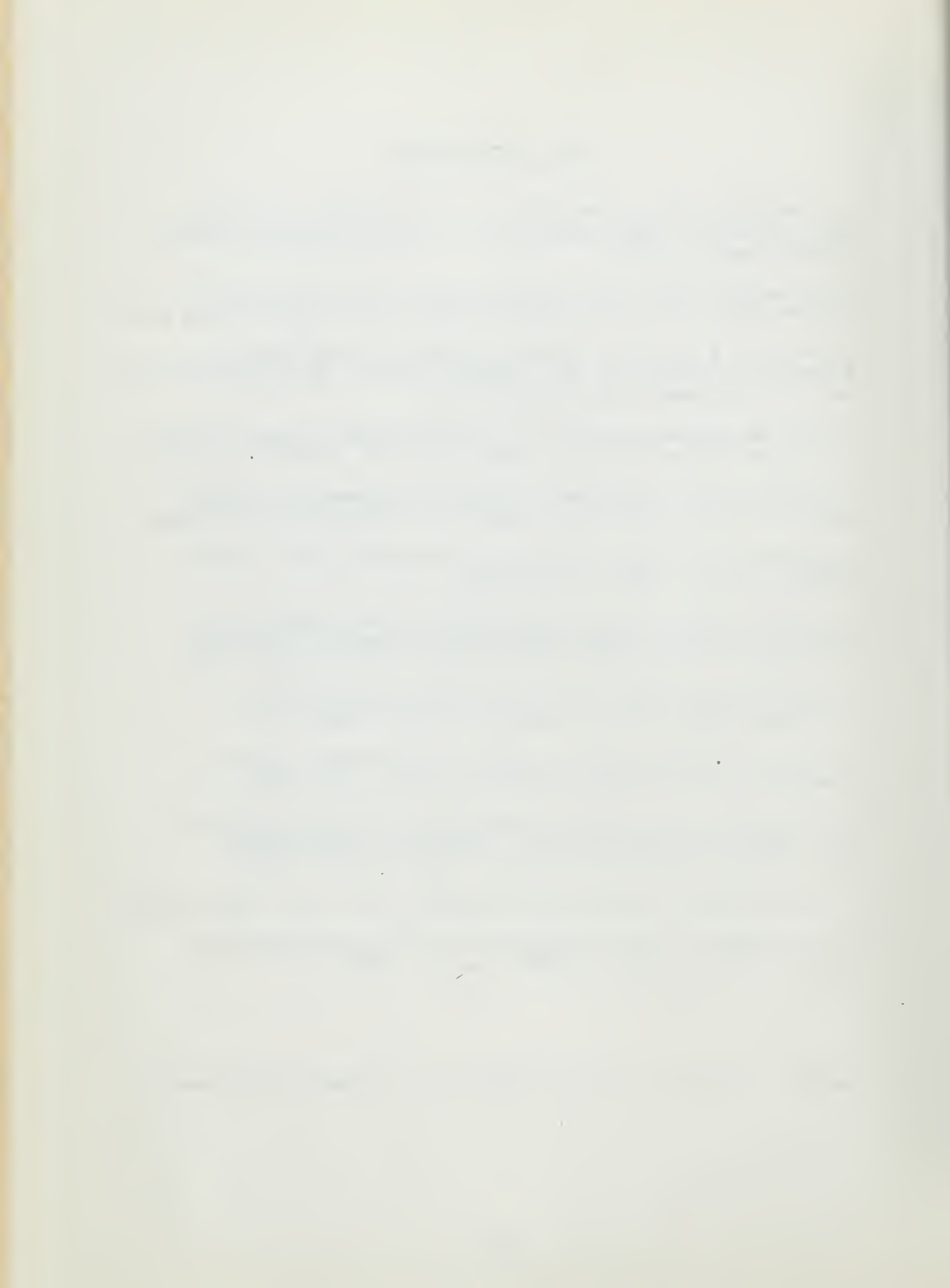


## VII. BIBLIOGRAPHY

1. Abkowitz, M.A., "Seakeeping Considerations in Design and Research," paper presented to the New England Section SNAME, January, 1957.
2. Abkowitz, M.A., and Paulling, J.R., "The Ship Model Towing Tank at M.I.T.," Trans. SNAME, vol. 61, 1953, pp 65-97.
3. Heller, S.R., Jr., "Wave Geometry for Longitudinal Strength," Journal of the American Society of Naval Engineers, vol. 66, November 1954, pp 925-938.
4. Korvin-Kroukovsky, B.V., "Investigation of Ship Motions in Regular Waves," Trans. SNAME, vol. 63, 1955, pp 386-435.
5. Lewis, E.V., "Ship Model Tests to Determine Bending Moments in Waves," Trans. SNAME, vol. 62, 1954, pp 426-490.
6. Lewis, E.V., "Ship Speeds in Irregular Seas," Trans. SNAME, vol. 63, 1955, pp 134-202.
7. Lewis, E.V., "Preliminary Study of the Influence of Controlled Fins on Ship Pitching and Heaving," Stevens Institute of Technology ETT Note No. 379, February 1957.
8. Lewis, F.M., "The Inertia of Water Surrounding a Vibrating Ship," Trans. SNAME, vol. 37, 1929, p 1.
9. Lutzi, P.C. and Kimball, E.D., "Ship Model Bending Moments in Waves," M.S. Thesis, M.I.T., May, 1957.
10. Pournaras, U.A., "Pitch Reduction with Fixed Bow Fins on a Model of the Series 60, 0.60 Block Coefficient," David Taylor Model Basin Report 1061, October 1956.
11. Seward, H.L., "Marine Engineering," vol. II, 1944, p 136.
12. Weinblum, G., and St. Denis, M., "On the Motions of Ships at Sea," Trans. SNAME, vol. 58, 1950.

\*SNAME - Society of Naval Architects and Marine Engineers







VIII. APPENDIX



## APPENDIX A

### Details of Procedure

As stated in the procedure, some means was necessary for cross-referencing the wave profile and bending moment tapes. The electric eye in the middle of the tow tank was connected to one channel of the Brush oscillograph in series with a six volt battery. This was a normally open circuit which closed only when the electric eye was tripped by a small piece of tape attached to the upper tow cord. This signal was indicated by the pen on one channel of the oscillograph. Then during each run, one person would simultaneously depress the manual marker buttons on the wave profile recorder and the bending moment recorder. Knowing the distance (physically measured) between the wave profile capacitance probe and the model at the time of tripping of the electric eye, it was possible to advance the recorded wave profile and ascertain the wave profile at the model for the bending moment recorded opposite the electric eye signal on the tape.



APPENDIX B

Equipment Data

<u>Item</u>	<u>Recorded Quantity</u>	<u>Source of Equipment</u>
1. Sanborn Recorder, single channel, Model 127, serial 396	Speed	MIT Tow Tank
2. Sanborn Recorder, single channel, Model 127, serial 935	Wave Profile	MIT Tow Tank
3. Brush Universal Analyzer, Model BL-320, serial 315	Strain Gage Input	Boston Naval Shipyard
4. Brush Direct Inking Oscillograph, two channel, Model BL-222, serial 42	Bending Moment & Electric Eye Signal	Boston Naval Shipyard
5. Berkley Eput Meter Model 554B	Speed	MIT Tow Tank
6. Berkley Integrator Model 1720	Speed	MIT Tow Tank
7. Heathkit Audio Generator Model AG-7	Speed	MIT Tow Tank



## APPENDIX C

### Summary of Data and Calculations

#### 1. Model and Ship Principal Dimensions

a. Type: Destroyer

b. Scale Ratio: 70

	<u>Model</u>	<u>Ship</u>
c. Displacement (full load)	24.91 lbs	3923 tons
d. Length overall (LOA)	5.98 ft	418'-5"
e. Length between perp. (LBP)	5.81 ft	407'-0"
f. Beam (at frame 112)	6.42 ft	44'-11 $\frac{1}{2}$ "
g. Draft (full load)	2.48 in	14'-6"
h. Depth (midships)	4.32 in	25'-3"
i. Block Coeff. ( $C_B$ )	0.517	0.517
j. Long. Prismatic Coeff. ( $C_p$ )	0.625	0.625
k. Neutral Axis (midships)	2.32 in	13.5 ft
l. Vertical C.G. (KG)	2.72 in	15.87 ft
m. Long. C.G. (LCG)	1.17 in aft	6.81 ft aft
n. Inertia Moment of midship Section	-	113,009 ft <sup>2</sup> -in <sup>2</sup>
o. Long. metacentric height	171.0 in	996.0 ft

#### 2. Computed Data

a. Two noded vertical natural frequency of bare hull	10.70 vps	1.28 vps
b. Radius of gyration	17.4 in	-
c. Natural pitching period	0.64 sec	-





d. Still water bending moment	19.0 in-lb (hogging)	
e. Maximum hogging bending moment using $1.1 \sqrt{L}$ trochoidal wave	80.5 in-lb	71,863ft-tons
f. Maximum sagging bending moment using $1.1 \sqrt{L}$ trochoidal wave	61.2 in-lb	54,696ft-tons



## APPENDIX D

### Sample Calculations

#### 1. Determination of the Two-Noded Vertical Natural Frequency of the Hull

a. The modified Schlick formula as proposed by Burrill in reference (11) was used.

$$N = \frac{\phi}{\sqrt{\left(1 + \frac{B}{2d}\right) (1+r)}} \sqrt{\frac{I}{\Delta L^3}}$$

where:

N = frequency in v.p.m.

I = moment of inertia of midship section in ft<sup>4</sup>

$\Delta$  = displacement in tons

L = LBP in feet

B = beam in feet

d = draft in feet

r = shear correction factor

D = molded depth in feet

a = B/D

$\phi$  = 2,400,000 as determined by Burrill

$$r = \frac{3.5D^2(3a^3 + 9a^2 + 6a + 1.2)}{L^2(3a + 1)}$$

$$r = 0.1219$$

$$N = \frac{2,400,000}{\sqrt{\left(1 + \frac{44.96}{2 \times 14.5}\right) (1.122)}} \times \sqrt{\frac{113,009}{144 \times 3923 \times 407^3}}$$

$$N = 77 \text{ v.p.m. or } 1.28 \text{ v.p.s. for ship}$$

$$N = 1.28 \sqrt{70} = 10.70 \text{ v.p.s. for model}$$



## 2. Determination of the Additional Inertia Mass of the Model

a. The formula as proposed by F. M. Lewis in reference (8) was used.

$$M = \frac{1}{2} C \times J \times \pi \times B^2 \times w$$

where:

M = additional inertia mass/  
unit length

C = inertia coefficient for  
each section

J = long. inertia coeff. for  
length/beam ratio of model

B = half beam

w = weight per unit volume of  
fluid

$$\text{Length/beam} = 407/44.96 = 9.05$$

Using this value of length/beam, reference (8) was used to obtain a "J" value of 0.84.

By use of the body plan and reference (8), values of "C" were determined as follows:

Station	C	M (lb/ft)
0	0.00	0.00
2	0.92	7.85
4	0.92	7.85
6	0.96	8.20
8	1.01	8.62
10	1.06	9.05
12	1.04	8.88
14	0.97	8.28
16	0.80	6.83
18	0.40	3.42
20	0.00	0.00

$$\text{Note: } M = \frac{1}{2} \times 0.84 \times 3.14 \times \frac{44.96^2}{2 \times 70} \times 62.4 \times C$$

$$M = 8.54 \times C$$



b. For the purposes of the Aluminum Flexure Bar size calculations it was assumed that the calculated additional inertia mass for each half could be replaced by a concentrated weight placed at the respective center of gravity.

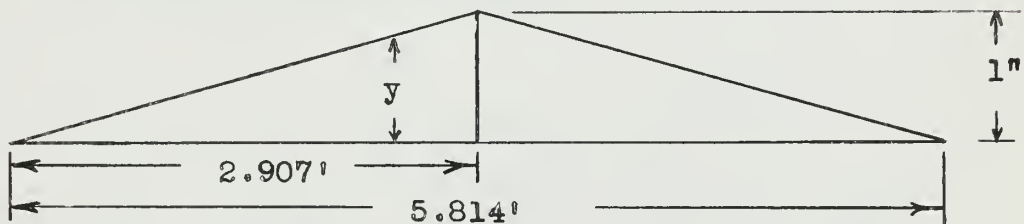
These weights and location are as follows:

Forward Half	21.53 lb. @ 1.279 ft. fwd Ø
After Half	18.57 lb. @ 1.112 ft. aft Ø

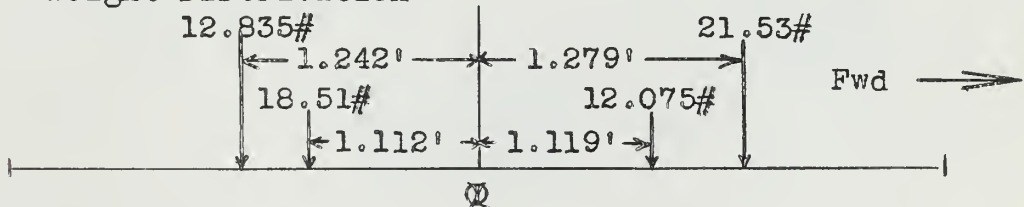
### 3. Determination of the Aluminum Flexure Bar Size

A method proposed by Prof. F. W. Lewis was used to calculate a deflection curve and from it the required bar size for a given natural frequency.

#### a. Assumed Deflection Curve

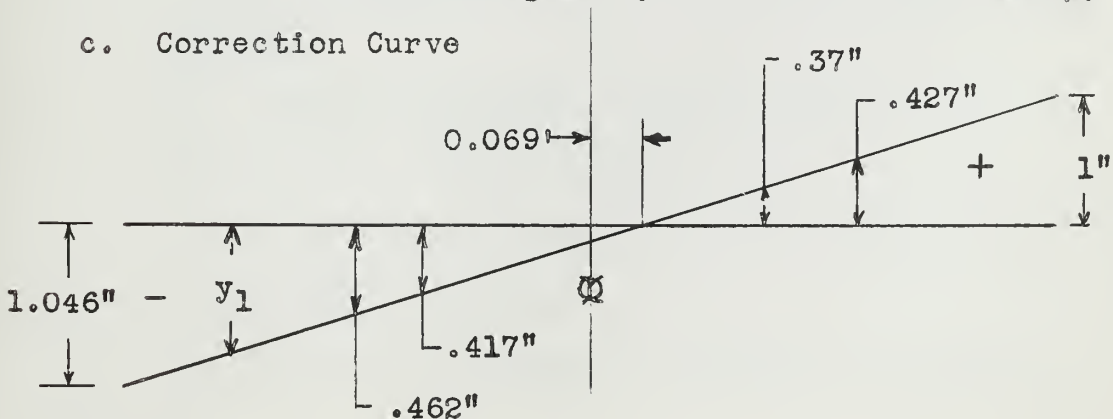


#### b. Weight Distribution



The center of gravity is at 0.069 ft. fwd Ø

#### c. Correction Curve







d. Correction Factors

$$C_0 = \frac{\sum y W}{\sum W} = \frac{7.36 + 11.46 + 7.42 + 12.05}{65.01} = .589$$

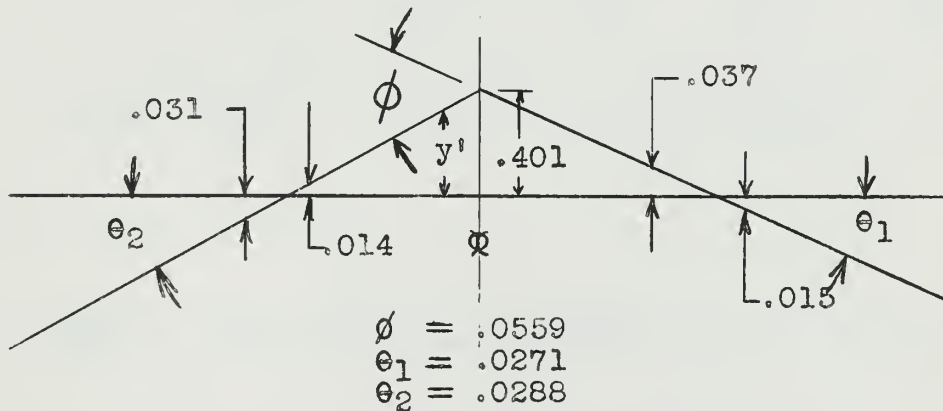
$$C_1 = \frac{\sum W y y_1}{\sum W y_1^2} = \frac{-3.41 - 4.77 + 2.75 + 5.15}{2.73 + 3.21 + 1.65 + 3.93} = -.033$$

Let the ordinates of the corrected deflection curve be  $y'$ , where

$$y' = y - C_0 - C_1 y_1$$

@ W = 12.835	$y' = -.031$
W = 18.51	$y' = .014$
W = 12.075	$y' = .037$
W = 21.53	$y' = -.015$

e. Corrected Deflection Curve



f. Energy Calculation

Symbols

PE = Potential Energy in foot-pounds

KE = Kinetic Energy in foot-pounds

$h$  = unsupported length of bar = 3 inches = 0.25 feet

$W$  = weight in pounds

$w$  = circular frequency in radians per second



x = displacement in feet

J = polar moment of inertia in pounds-feet<sup>2</sup>

θ and φ are angles as shown on diagram in radians

I = moment of inertia of the bar in feet<sup>4</sup>

E = modulus of elasticity = 10 x 10<sup>6</sup> psi. for Al.

$$KE = \sum \frac{W}{2g} w^2 x^2 + \sum \frac{J}{2g} w^2 \theta^2$$

$$J = WL^2/12 \quad \text{for Fwd Half; } J = 33.61 \times 6.25/12 \\ = 17.51 \text{ lb.ft.}^2$$

$$\text{for Aft Half; } J = 31.34 \times 6.25/12 \\ = 16.32 \text{ lb.ft.}^2$$

$$KE = \frac{12.835}{64.4} w^2 \frac{(.031)^2}{144} + \frac{18.51}{64.4} w^2 \frac{(.014)^2}{144} + \frac{12.075}{64.4} w^2 \frac{(.037)^2}{144} + \\ \frac{21.53}{64.4} w^2 \frac{(.015)^2}{144} + \frac{17.51}{64.4} w^2 \frac{(.0271)^2}{144} + \frac{16.32}{64.4} w^2 \frac{(.0288)^2}{144}$$

$$KE = 4.14 \times 10^{-4} w^2$$

$$PE = \frac{EI\phi^2}{2h} = \frac{144 \times 10^7 \times I \times (.0559)^2}{2 \times .25} = 9 \times 10^6 I$$

$$PE = KE \quad \text{therefore, } 4.14 \times 10^{-4} w^2 = 9 \times 10^6 I$$

It was determined that the highest frequency of encounter would be about 3.5 cps. With a desired factor of safety of five, the required natural frequency of the bar would therefore be 17.5 cps.

$$w = 2\pi f = 35\pi = 110, \quad w^2 = 12,100$$

$$I = \frac{4.14 \times 10^{-4}}{9 \times 10^6} \times 12,100 \times 144 \times 144 = .0116 \text{ in}^4$$



$$I = bt^3/12, \text{ if } b = 1 \text{ inch, } t^3 = .13884$$
$$t = .52 \text{ inches}$$

An aluminum bar 1 inch wide by 1/2 inch thick that had been used in reference ( 9 ) was available. It was decided that this bar was satisfactory.



#### 4. Determination of the Radius of Gyration

a. The model was suspended by two springs of equal spring constant at equal distances from the longitudinal center of gravity. It was then made to oscillate in air, first in heaving, then in pitching; and the time for 30 cycles in each motion was measured by stop watch. The following formula was then used to determine the radius of gyration:

$$k_y = \frac{T_{pa}}{T_{ha}} \times \frac{b}{2}$$

where:

$k_y$  = radius of gyration in inches

$T_{pa}$  = pitching period in air in sec.

$T_{ha}$  = heaving period in air in sec.

$b$  = distance between springs in inches

$$k_y = \frac{24.75}{46.00} \times \frac{64.7}{2}$$

$$k_y = 17.4 \text{ inches}$$

#### 5. Determination of the Natural Pitching Period of the Model

a. The following formula as proposed by E. V. Lewis in reference (6) was used:

$$T_p = 2\pi \sqrt{\frac{J_L C_{vi}}{g \nabla GM_1}}$$

where:

$J_L$  = long. mass moment of inertia

$C_{vi}$  = coefficient of virtual inertia or  $(1 + k_{yy})$

$$\text{But } J_L = \nabla \rho k_y^2$$

$k_y$  = radius of gyration as determined above

$k_{yy}$  = coeff. of ascension to inertia

$GM_1$  = long. metacentric height

$$\therefore T_p = 2\pi \sqrt{\frac{k_y^2 C_{vi}}{g GM_1}}$$

From reference (12), a value of  $k_{yy} = 1.295$  was determined

$$T_p = 2\pi \sqrt{\frac{17.4^2 \times 2.295}{386 \times 171}} = 0.64 \text{ seconds}$$





## APPENDIX E

### Drawings and Photographs

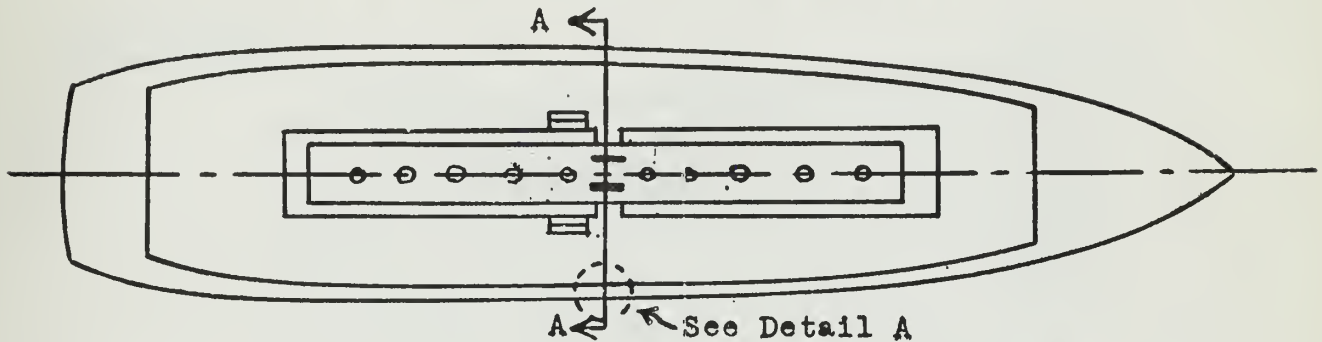
#### Figure

- IX. Sketch of Model Showing Flexure Bar Installation
- X. Sketch of Model Showing Bow Fin Installation
- XI. Diagram of Strain Gage Installation
- XII. Method of Strain Gage Calibration
- XIII. Photograph of Midship Section Showing Flexure Bar and Towing Bracket
- XIV. Photograph of Instrument Setup
- XV. Photograph of Model Fully Rigged in Tow Tank
- XVI. Photograph of Bow with Anti-Pitching Fins Installed

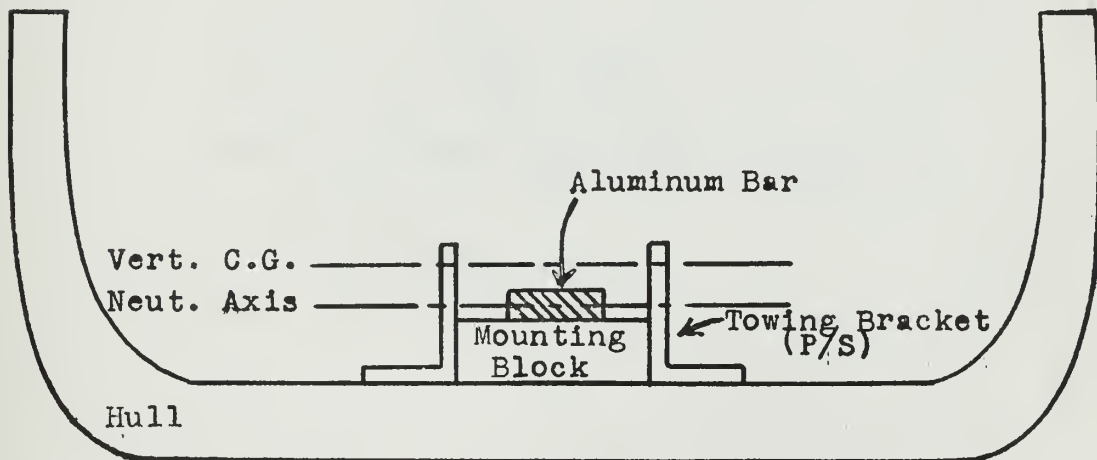


FIGURE IX

Sketch of Model Showing Flexure Bar Installation



Plan View



Sect. AA

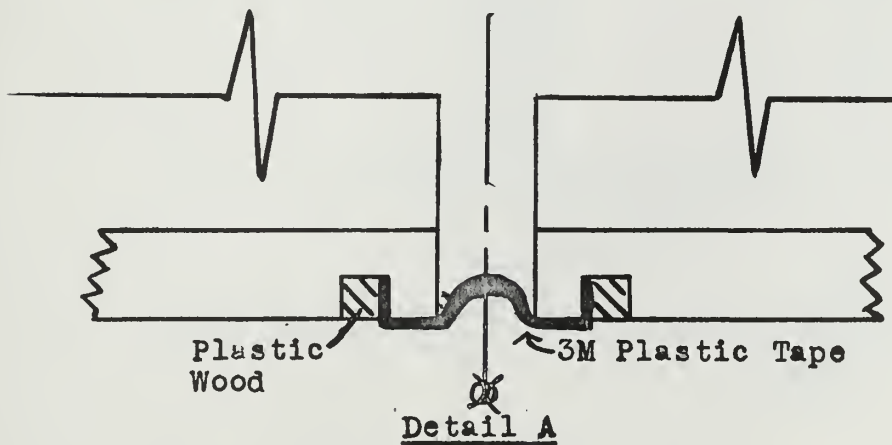




FIGURE X

Sketch of Model Showing Bow Fin Installation

Sheet Metal  
Cover Plate

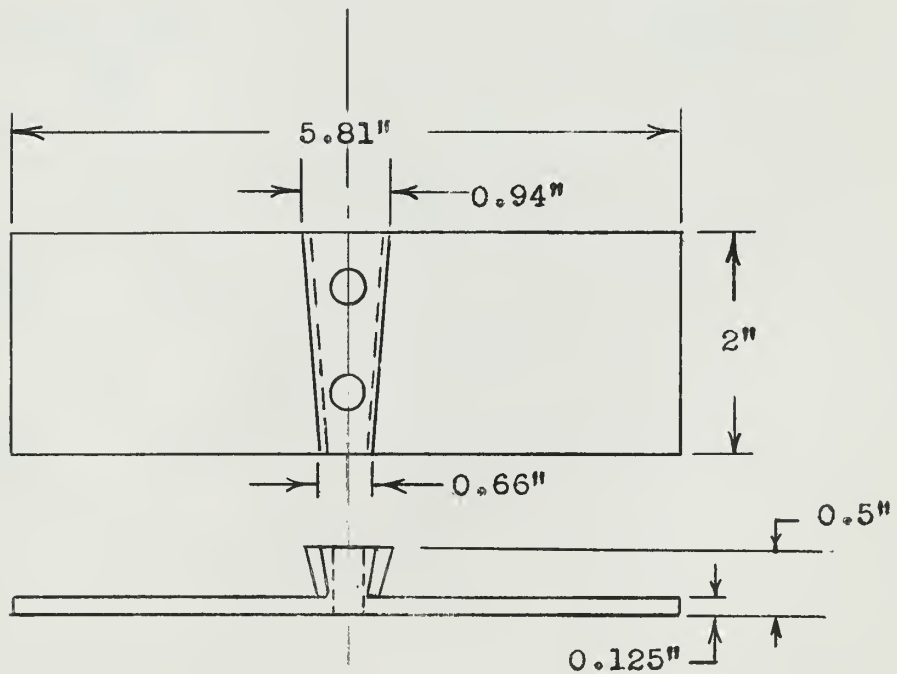
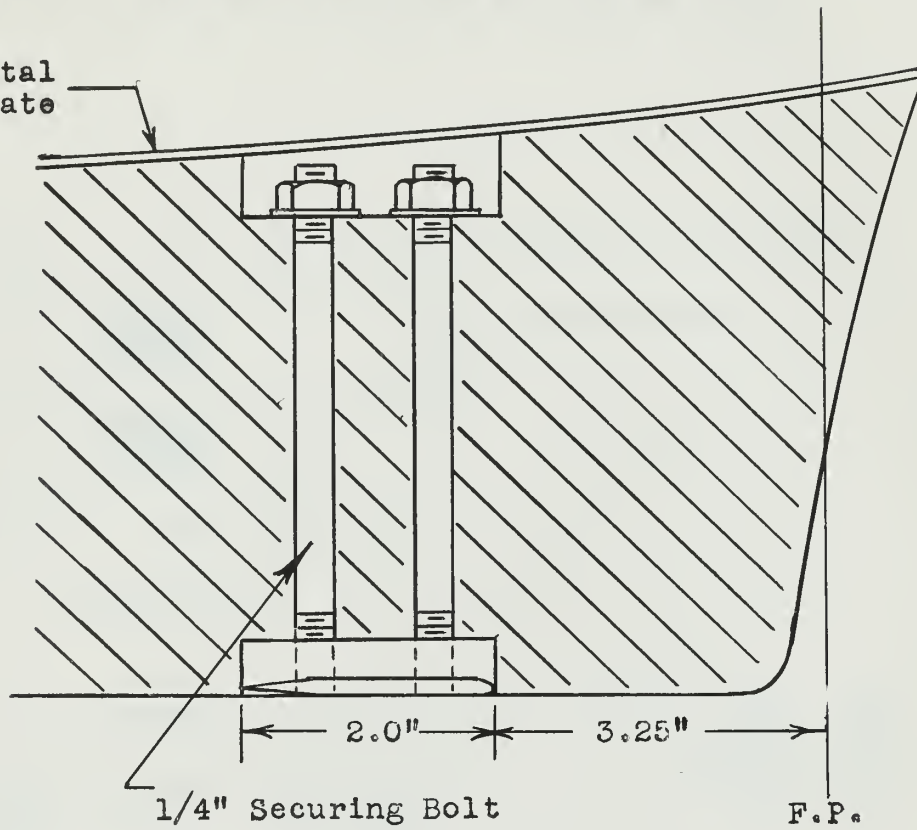




FIGURE XI

Diagram of Strain Gage Installation

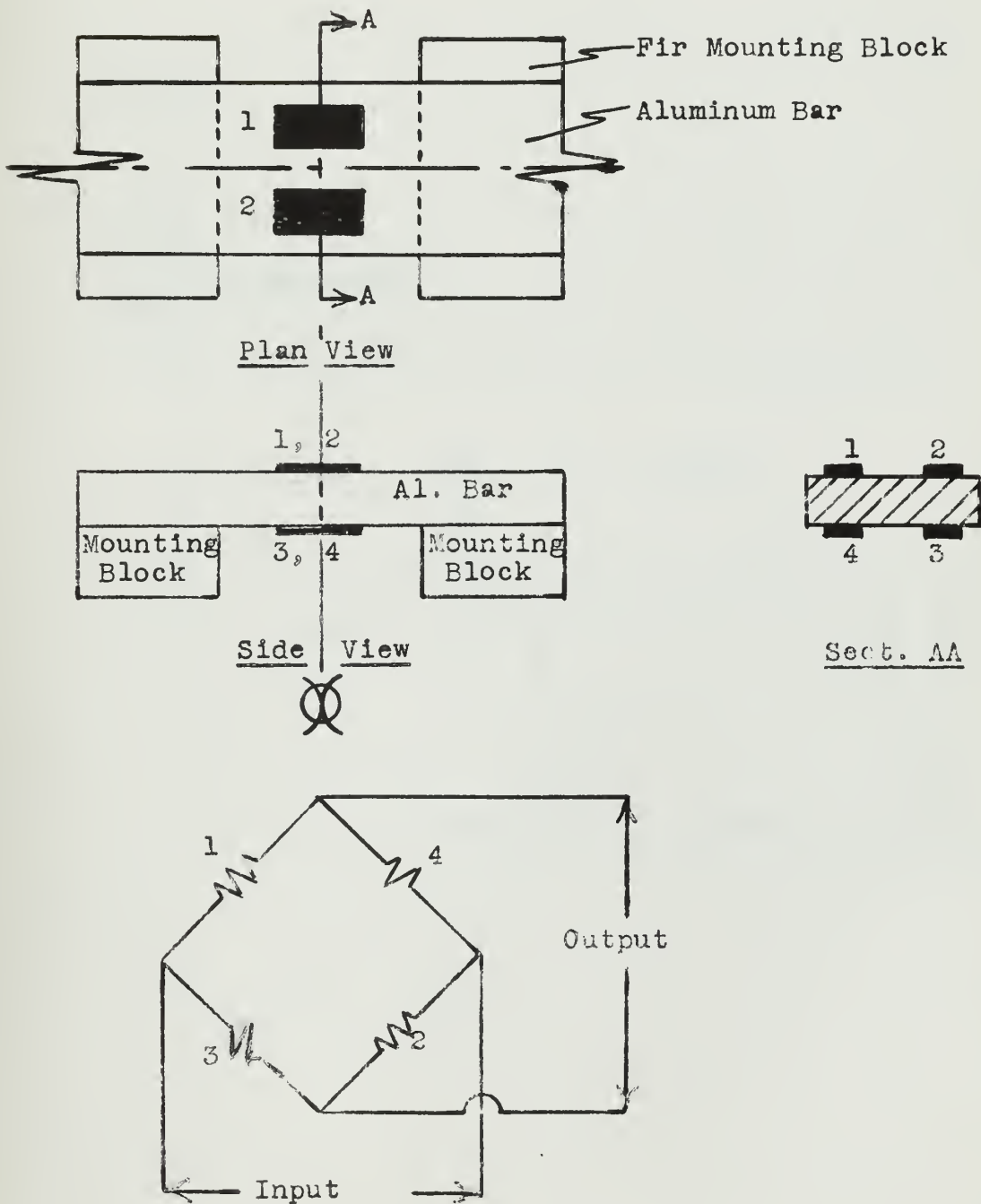
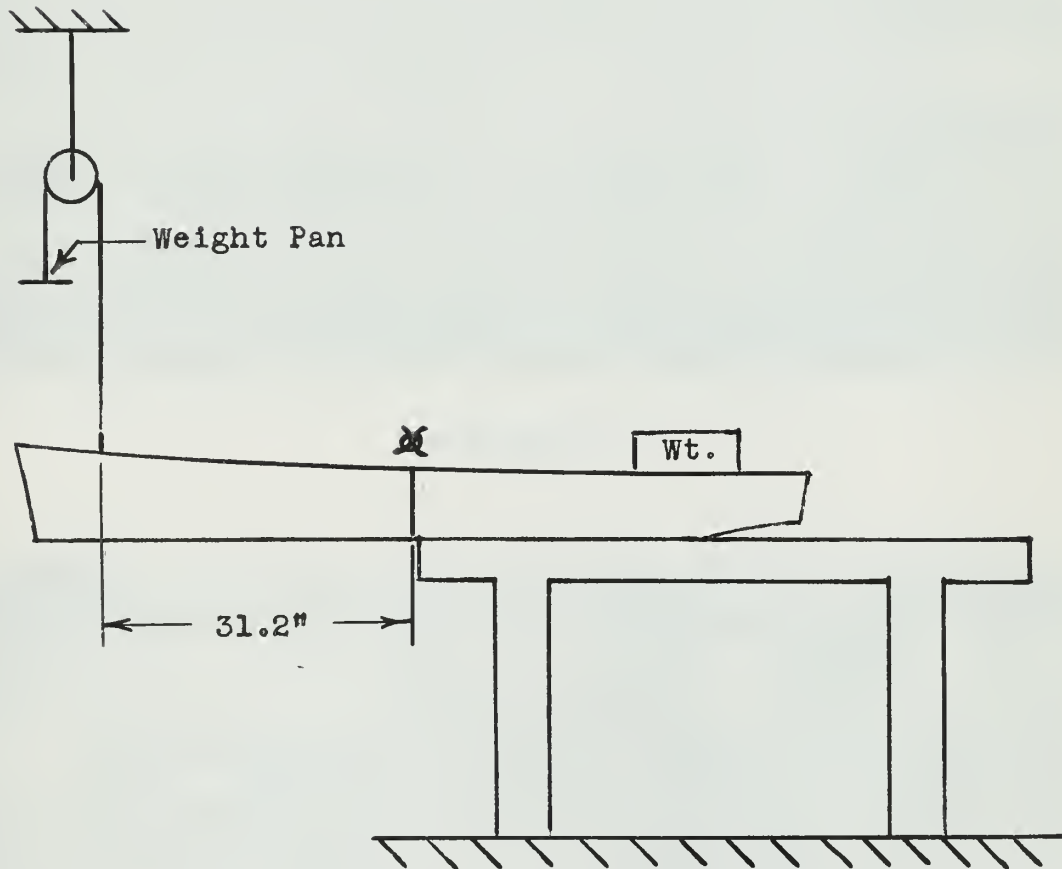






FIGURE XII

Method of Strain Gage Calibration





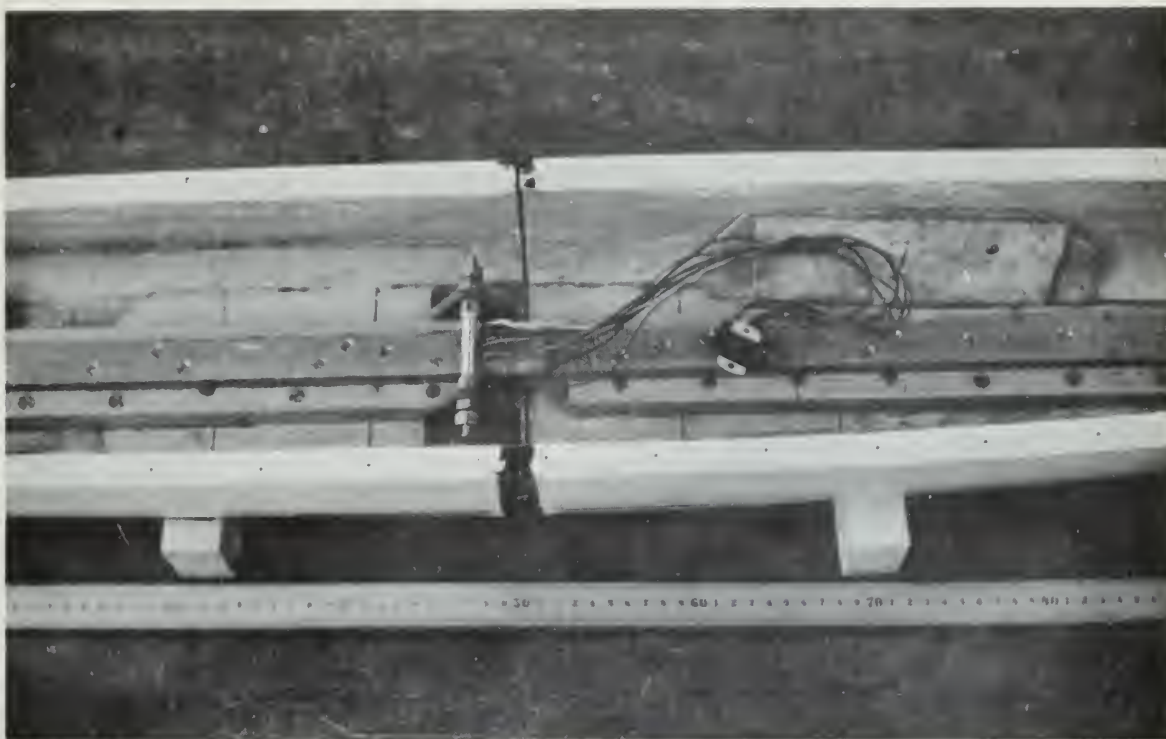


FIGURE XIII

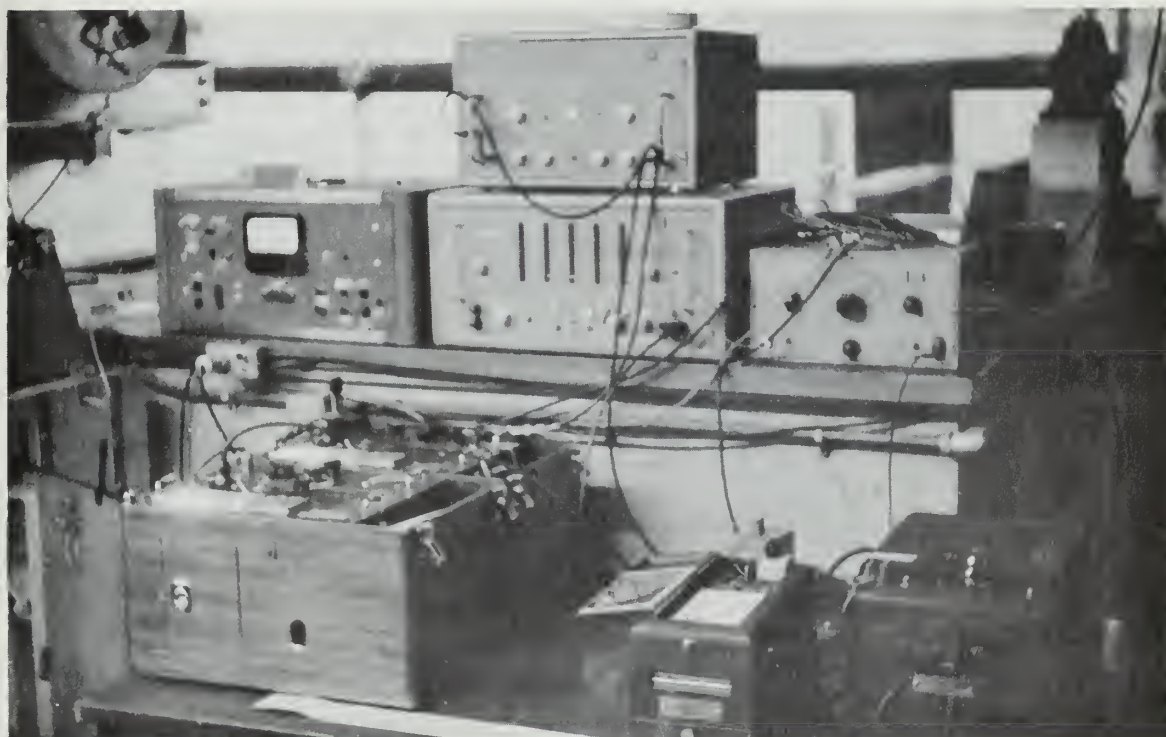


FIGURE XIV



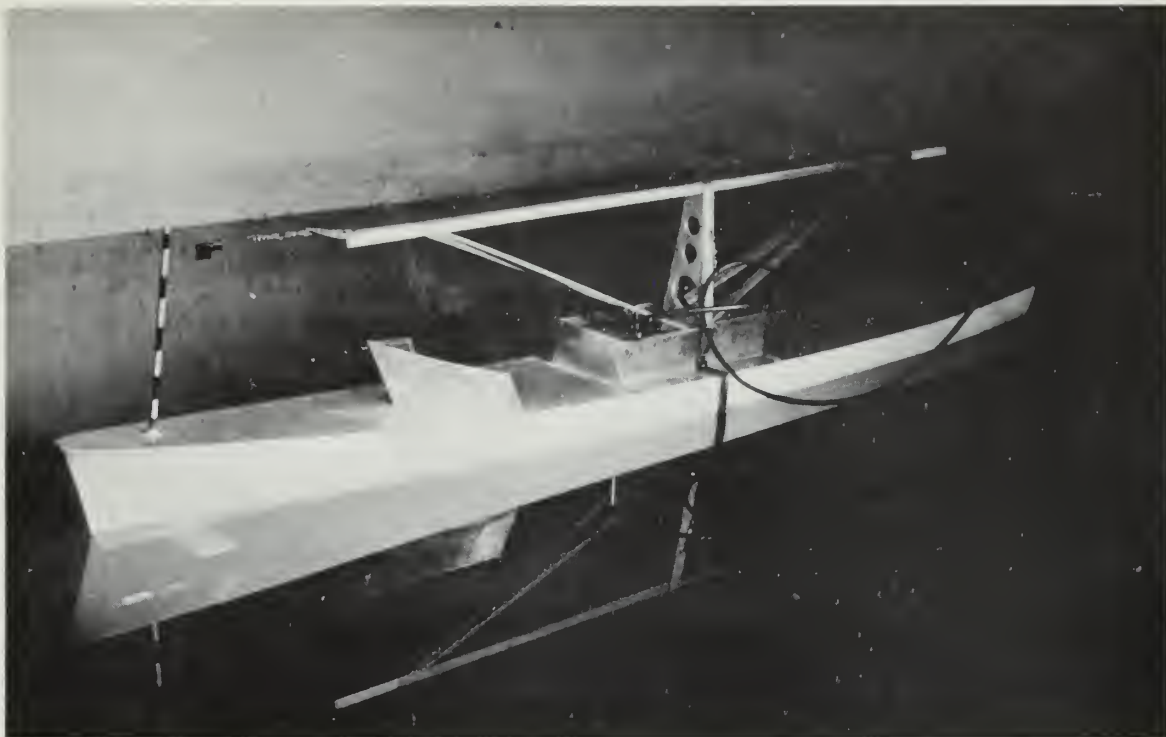


FIGURE XV



FIGURE XVI



APPENDIX F  
Original Data

Table

I	Still Water Speeds and Towing Forces
II	Bending Moments and Model Speeds in Waves
III	Location of Wave Profile





TABLE I

Original Data

Still Water Speeds and Towing Forces

Without Fins

<u>Tow Force</u> <u>(lbs)</u>	<u>V<sub>s</sub> (ship)</u> <u>(kts)</u>	<u>V<sub>s</sub> (model)</u> <u>(kts)</u>
0.884	10	1.197
1.832	15	1.793
3.442	20	2.390
7.540	27	3.227

With Fins

1.228	10	1.197
2.114	15	1.793
3.840	20	2.390
7.982	27	3.227



TABLE II

Original Data

Bending Moments and Model Speeds in Waves

Run	$\lambda/L$	a	$V_s$ (ship) (kts)	$V_v$ (model) (kts)	Maximum Bending Moment in Excess of Still Water(in-lb)	
					Hogging	Sagging
** NO FINS **						
1A	1.08	L/22	15	0.854	35.4	45.7
1B	1.00	L/20	15	0.912	34.4	41.2
2	1.00	L/21	20	1.312	32.9	45.7
3A	0.98	L/19	27	2.043	26.9	55.8
3B	0.99	L/20	27	1.956	27.0	54.0
4A	0.99	L/20	10	-	30.0	41.7
4B	0.97	L/19	10	0.352	30.2	40.2
5	0.76	L/19	10	0.888	22.7	34.9
6	0.73	L/18	15	0.900	24.1	32.6
7	0.72	L/17	20	1.839	25.9	33.2
8	0.70	L/17	27	3.100	20.2	41.5
9	1.31	L/23	27	2.540	24.6	52.2
10	1.31	L/23	20	1.558	20.4	53.2
11	1.32	L/22	15	0.746	26.0	37.3
12	1.31	L/23	10	0.374	25.5	35.2
** WITH FINS **						
13	1.27	L/19	27	1.359	27.7	53.6
14A	1.26	L/18	20	0.720	35.6	50.3
14B	1.27	L/19	20	0.646	34.4	46.6



Run	$\lambda/L$	a	$V_s$ (ship) (kts)	$V_v$ (model) (kts)	Maximum Bending Moment in Excess of Still Water(in-lb)	
					Hogging	Sagging
15A	1.28	L/19	15	-	34.9	38.2
15B	1.28	L/20	15	0.283	34.1	38.3
16	1.29	L/20	10	0.400	30.0	47.5
17	1.04	L/19	10	0.084	40.1	30.7
18	1.04	L/21	15	0.347	30.1	37.1
19	1.04	L/20	20	0.633	37.5	39.5
20	1.05	L/21	27	1.444	26.6	59.6
21	0.79	L/23	27	2.698	25.9	46.6
22	0.79	L/22	20	1.441	25.2	34.4
23	0.78	L/22	15	0.561	24.5	28.5
24	0.78	L/22	10	0.592	28.4	26.9

Note: (1) Theoretical wave height (a) for all runs was L/20.

(2) Theoretical $\lambda/L$	Runs
0.75	5-8, 21-24
1.00	1-4, 17-20
1.25	9-16



TABLE III

Original DataLocation of Wave Profile

<u>Run</u>	<u>Bending Moment at electric eye mark (in-lb)</u>		<u>% Total Bending Moment</u>		<u>Nodal Posit Aft of <del>X</del> as % <math>\lambda</math></u>
	<u>Hogging</u>	<u>Sagging</u>	<u>Hogging</u>	<u>Sagging</u>	
1B	51.7	-	97.3	-	6.0
2	5.0	-	9.7	-	90.6
4A	43.2	-	88.3	-	47.0
4B	45.1	-	92.0	-	35.0
5	-	16.1	-	100.0	57.0
6	41.8	-	97.7	-	93.5
7	-	10.1	-	70.0	33.4
8	-	22.7	-	100.0	12.0
10	7.0	-	17.8	-	69.3
12	-	5.5	-	33.3	60.0

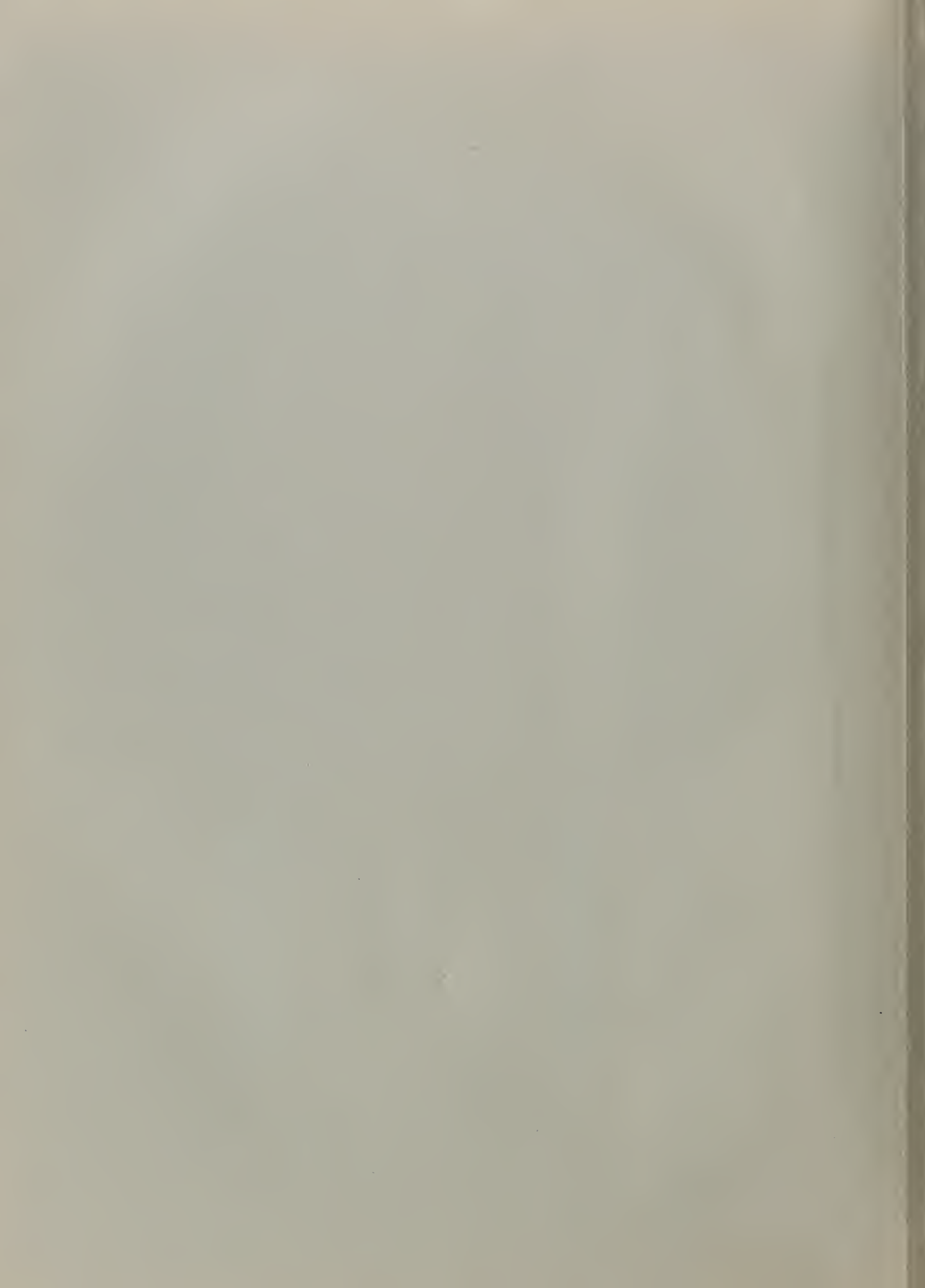














thesM8227

The influence of anti-pitching fins on s



3 2768 001 91690 1

DUDLEY KNOX LIBRARY